Solid-liquid slip from a transition state theory lens

Nicolas G. Hadjiconstantinou

*Department of Mechanical Engineering Massachusetts Institute of Technology Cambridge,
Massachusetts 02139, USA*

Using molecular dynamics simulations, we assess the ability of transition state theory
(TST) to describe the slip length of a simple liquid in contact with a simple solid under
a wide range of pressures and temperatures, as well as other system parameters. In the
linear regime of low shear rates that is of practical interest, TST leads to an Arrhenius-
type expression with temperature and density-dependent pre-exponential factors. Extensive
comparison with molecular dynamics simulation results shows that the resulting model can
fit simulation data very well. Of particular note is the model's ability to capture the strong
dependence of slip on pressure; according to the model, this dependence originates in the
work of expansion associated with hole formation in the activated state and appears in the
Arrhenius exponent as part of the Gibbs free energy of activation. We also show that under
certain conditions, the model reduces to particularly simple expressions for describing the
slip as a function of the system thermodynamic state.

I. INTRODUCTION

We have recently marked the bicentennial anniversary of the Navier slip condition [1]

$$u_s = \beta \frac{\partial u}{\partial \eta} \tag{1}$$

describing the slip velocity u_s at the fluid-solid boundary as a function of the gradient of the
tangential flow velocity in the direction normal to the boundary, η. In contrast to the case of dilute
gases, where first principles approaches [2–4] allow the exact calculation of the slip length, β,
determination of the latter remains a significant challenge for dense liquids [2]. Although slip can be
measured experimentally, including via computer experiments such as molecular dynamics (MD)
simulations provided an accurate interaction potential for describing the solid-liquid interface is
available, predictive models which relate the slip length to the system parameters and thermody-
namic state have yet to be fully developed.

Notable progress in this respect has been made by Bocquet and collaborators [5–7] who used
Green-Kubo (GK) theory to obtain a model for the slip length in simple fluids in terms of the
fluid structure factor in the first liquid layer (FLL) [8] in contact with the solid and the charac-
teristic timescale associated with the solid-liquid force autocorrelation integral. Unfortunately, no
models exist for connecting these quantities to readily available system properties. Moreover, this
approach requires knowledge of the hydrodynamic wall location [9], which in some cases may be
significantly different from the actual wall location [10] and for which no reliable predictive model
exists [2,10].

A different class of approaches relies on mechanistic models of the solid-liquid interaction
and resulting slip process. Notable approaches include the work by Lichter and collaborators
[11,12] who developed a variable density Frenkel-Kontorova equation for this purpose and showed
that its numerical solutions are in qualitative agreement with MD simulations. The author of

this article has shown [13] that by using a simpler model for the fluid-fluid interactions in the above formulation, a much more tractable governing equation results, which readily lends itself to numerical solutions and even analytical treatments in some limiting cases. This latter model was shown [13] to be in good quantitative agreement with MD simulations. Unfortunately, these mechanistic models require knowledge of the atomistic-level friction coefficient, which is not known in general.

A simpler but potentially powerful approach for modeling the slip process relies on transition state theory (TST) [14], in the sense pioneered by Blake [15], to model the motion of contact lines. This approach is motivated by the success enjoyed by Blake's "molecular kinetic theory" in modeling contact-line motion [16–19]. The consistency between various aspects of the more general slip phenomenon and TST predictions has been pointed out by a number of researchers [12,20–24], making a strong case that, at least under certain conditions which need to be determined, TST might be able to model slip processes in a predictive sense.

The most important drawback associated with simple TST-based models is the simplified treatment of the physics governing slip motion, resulting from the assumption that the latter is a result of a single, well-defined thermally activated process. With this in mind, the current work aims to provide a deliberate investigation of the ability of this class of models to describe slip quantitatively. Although our investigation spans a wide range of conditions and fluid-solid system parameters, we pay particular attention to the strong dependence of slip on pressure (see data in [5], for example), which, in our opinion, has not received sufficient attention to date.

To this end, in Sec. II we use Eyring's reaction rate theory to develop a more complete expression for the slip length compared to the simple model presented in [24]. In Sec. III, we use MD simulations to validate this relation extensively, in order to provide a better understanding of the strengths and limitations of this approach as a way of assessing its potential of being developed into a reliable and perhaps predictive model of slip. This comparison is limited to the linear limit of low shear rate since, as we explain in more detail later, essentially all problems of practical interest fall in the small driving force regime. Discussion of our results, as well as some conclusions, can be found in Sec. IV.

II. MODEL FORMULATION

A. TST for liquid slip

In the interest of simplicity, we consider a planar, stationary solid wall parallel to the $x - y$ plane in contact with a liquid that occupies the $z > 0$ dimension. The liquid is subject to simple shear, resulting in a shear stress $\tau_{xz} = \mu \dot{\gamma}$, where $\dot{\gamma}$ denotes the shear rate and μ the liquid viscosity. The system temperature and pressure are given by T and P, respectively.

The slip velocity in the x direction, u_s, can be identified with the velocity of the FLL [2] in contact with the solid as a result of an applied shear stress. A model for this motion can be constructed by extending the theory by Eyring and coworkers for viscous flow [25,26] by envisioning liquid atomic motion at the FLL to be a result of infrequent hops between unoccupied sites, or "holes," on the solid surface. These hops are infrequent due to the large potential barrier associated with escaping the "cage" formed by the surrounding atoms, which in this case are both on the liquid and the solid side. Here, we note that transition-state-theory-based approaches to transport in liquids were also developed by Frenkel [27], and that these ideas were applied to slip by Tolstoi [28] (see [29] for a critique of Tolstoi's paper).

Using these ideas, we write [24]

$$u_s = \ell(\kappa^+ - \kappa^-), \tag{2}$$

where ℓ denotes the jump length between available sites and $\kappa^{\pm}$ the hopping rate in the positive and negative x direction. These rates differ because the applied shear stress results in a net force on fluid particles in the x direction, thus tilting the potential landscape and introducing an asymmetry in the

potential barrier. Using reaction-rate theory [26] to describe the rates $\kappa^\pm$, we obtain

$$\kappa^\pm = \frac{k_B T}{h} \exp\left(-\frac{\Delta G \mp \frac{1}{2} f_x \ell}{k_B T}\right), \tag{3}$$

where k_B denotes Boltzmann's constant, h is Planck's constant, ΔG is the per-atom difference in Gibbs Free Energy between the activated and equilibrium states, and $f_x = \tau_{xy}/\Sigma$ denotes the force on each fluid particle acting in the x direction as a result of the shear. In the above, Σ denotes the areal density—number of atoms per unit area—at the solid-liquid interface [8].

As discussed in [24], molecular-kinetic expressions such as Eq. (3) predict a nonlinear relationship of the form

$$u_s \propto \sinh\left(\frac{\mu \dot{\gamma} \ell}{\Sigma k_B T}\right) \tag{4}$$

between the slip velocity and the shear rate, which is in good agreement with MD simulations. Although this relation has received some interest [11,30,31], in what follows, we exclusively focus on the low-forcing (linear) limit $\dot{\gamma} \ll \Sigma k_B T/\ell \mu$, which is the most relevant one for applications of interest. This can be seen by noting that for a simple dense liquid of density $\rho \sim 1$, the condition for linearity simplifies to $\dot{\gamma} \ll 1$ in atomistic units [2], which is approximately equivalent to $\dot{\gamma} \ll 10^{11} s^{-1}$ in SI units. Clearly this requirement is met by the vast majority of real applications of interest.

In the linear limit as defined above, expression (3) simplifies to

$$u_s = \frac{\ell^2 \mu}{\Sigma h} \exp\left(-\frac{\Delta G}{k_B T}\right) \dot{\gamma}. \tag{5}$$

We follow Blake [15] in assuming that ΔG can be decomposed into a liquid-liquid interaction part, ΔG_{LL}, and a liquid-solid interaction part, ΔG_{LS}, with the former linked to the liquid viscosity via

$$\mu = \frac{h}{v_L} \exp\left(\frac{\Delta G_{LL}}{k_B T}\right), \tag{6}$$

where v_L denotes the liquid free volume [15]. Using this decomposition, we can write

$$u_s = \frac{\ell^2}{\Sigma v_L} \exp\left(-\frac{\Delta G_{LS}}{k_B T}\right) \dot{\gamma}. \tag{7}$$

Assuming a linear velocity gradient in the wall vicinity, as usual in slip-flow theory [2], we obtain

$$\beta = \frac{\ell^2}{\Sigma v_L} \exp\left(-\frac{\Delta G_{LS}}{k_B T}\right). \tag{8}$$

Relation (8) is a relatively simple expression for the slip length in the limit of small shear rate (linear conditions), which, as discussed above, should hold over a very wide range of shear rates, including those of practical interest. Working with the slip length, as opposed to the friction coefficient $\zeta = \mu/\beta$, has the advantage of eliminating the viscosity, with its quite complex dependence on the fluid state (e.g., temperature and pressure), from the final expression. We note that since u_s was calculated at the FLL location, the corresponding slip length is to be interpreted as measured from this location. This will be taken into account when comparing this relation with our MD simulation results.

We next proceed to develop Eq. (8) into a form that can be most readily compared with simulation results.

B. Thermodynamics of the activation barrier

Thermally activated phenomena with a simple constant activation barrier can be recognized from their signature exponential dependence on temperature, typically by plotting the natural logarithm of the reaction rate versus inverse temperature on an Arrhenius plot. In the case of Eq. (8), the numerator of the exponent

$$\frac{\Delta G_{LS}}{k_B T} = \frac{\Delta U - T\Delta S + P\Delta V}{k_B T} \tag{9}$$

is not a constant with respect to temperature as in classical TST problems. Moreover, v_L and Σ appear in Eq. (8) as pre-exponential factors that need to be taken into account. In other words, a classic Arrhenius plot will not suffice here.

In the above equation, ΔU, ΔS, and ΔV denote the per-atom energy, entropy, and volume difference between the activated (subscript a) and equilibrium states (subscript e), following the notation $\Delta I = I_a - I_e$, where $I \in \{U, S, V\}$. We also note that these quantities refer to the liquid-solid interaction and corresponding part of the Gibbs free energy with the subscript LS suppressed in the interest of simplicity. The expression $\Delta G_{LS} = \Delta U - T\Delta S + P\Delta V$ can be arrived at by starting from the corresponding expression for ΔG and separating each term into a liquid-solid and a liquid-liquid contribution. The latter are then eliminated via Eq. (6) after being grouped into ΔG_{LL}.

Of particular note is the role of pressure which contributes to ΔG_{LS} via the liquid volume change associated with formation of holes, which mediate the slip process, in analogy to the case of viscosity in a homogeneous dense liquid [26]. As a result, the pressure will feature as an independent variable in our plots.

To account for the pre-exponential factors, we use observations from previous studies which suggest power law behaviors for Σ [8] and v_L [26]. Coupled with the observation that ℓ is a mostly geometric quantity (primarily dependent on the solid density and structure), we rewrite Eq. (8) in the form

$$\ln\left(\frac{\beta}{T^\alpha \rho^\gamma}\right) = B + \frac{T\Delta S - \Delta U}{k_B T} - \frac{P\Delta V}{k_B T}, \tag{10}$$

where $B = B(\{\phi\})$ is a system constant. In this context, we will use the term system constant to refer to quantities that are fixed for a given system definition and do not depend on the thermodynamic state; in other words, quantities that do not depend on the temperature and pressure (and thus density) but can depend on the set of parameters that define the system of interest, $\{\phi\}$, which includes, for example, the solid density and structure, the various intermolecular interactions, molecular masses, etc.

As will be seen below, the MD data can be described very well by the empirically determined values $\alpha = 0.5$ and $\gamma = -0.5$, which will be used (held fixed) throughout this work.

III. COMPARISON WITH MOLECULAR DYNAMICS SIMULATIONS

We performed equilibrium and nonequilibrium MD simulations of a model system over a variety of conditions in order to validate the ability of Eq. (10) to describe slip data accurately over a wide range of conditions, while providing insight into slip behavior including potentially useful scaling arguments.

A. Molecular dynamics simulations

The proposed model is validated using MD simulation results from Couette flow simulations in a system comprising a dense liquid bounded by two fcc-structured walls in a slab geometry. Atomic

interactions were based on the generalized Lennard-Jones potential

$$u_{ij}(r) = 4\varepsilon_{ij}\left[\left(\frac{\sigma_{ij}}{r}\right)^{12} - C_{ij}\left(\frac{\sigma_{ij}}{r}\right)^{6}\right], \tag{11}$$

where r denotes the distance between atoms i and j. More details on the simulation setup can be found in Appendix A.

In what follows, we will use subscript s to denote solid atoms and their properties and l to denote liquid atoms and their properties. All quantities will be reported in nondimensional units using the characteristic time $\tau_{LJ} = \sqrt{m_l \sigma_{ll}^2/\varepsilon_{ll}}$, the characteristic distance σ_{ll}, and the potential well depth ε_{ll} associated with the liquid-liquid interaction. In all cases the slip reported is as calculated at the FLL location. It was obtained using a combined Green-Kubo and nonequilibrium analysis which takes into account the hydrodynamic wall location [10], as well as the distance between the wall and the FLL [8]; more details can be found in Appendix B. The liquid pressure $P = P(\rho, T)$ was obtained from the equation of state (EOS) of Gubbins *et al.* [32] using measured values of the bulk liquid density and temperature; using the pressure as measured directly from the MD simulation (normal force on the bounding walls) yields equivalent results (within a few percent).

B. Results

Before discussing our results in detail, we note that our simulations span a range of Wall numbers, $0.1 \lesssim \mathrm{Wa} \lesssim 1$; the latter, defined as $\mathrm{Wa} = \rho_s \varepsilon_{sl}/k_B T$, is the characteristic number governing liquid layering at the liquid-solid interface [8]; under this definition, negligible layering is observed for $\mathrm{Wa} \ll 1$ [8]. In other words, the Wall numbers studied here explore the range of small to moderate layering. It is noteworthy that, as will be seen below, no discontinuous behavior across variations in this parameter (and thus layering) is observed.

1. Variation of slip with density at fixed temperature

Figure 1 presents MD simulation results obtained by varying the liquid density in the range $0.53 < \rho < 0.92$ at fixed temperature. A variety of comparisons are shown to highlight the effect of wall density, temperature, and solid-liquid interaction strength.

Under the drastic, perhaps, assumption that ΔS, ΔV, and ΔU are sufficiently weak functions of density (pressure) for its effect to be negligible in these quantities, Eq. (10) simplifies to

$$\ln\left(\frac{\beta}{T^\alpha \rho^\gamma}\right) = c_1 - c_2 \frac{P}{k_B T}, \tag{12}$$

where c_1 and $c_2 = \Delta V$ are constants for each isothermal density sweep shown in the figure. To assess the validity of this model, Fig. 1 plots the LHS of (12) as a function of the ratio P/T, with $P = P(\rho, T)$ calculated from the liquid EOS as discussed in Sec. III A.

The top panel of Fig. 1 compares MD simulation results at fixed temperature $T = 1.5$ for three different solid-liquid interactions. Here and in what follows, ε_{sl} is varied independently of ε_{ss} and ε_{ll}; in other words, unless otherwise stated, ε_{ll} and ε_{ss} remain fixed at their nominal values of 1 and 4, respectively. The agreement between the model and the simulation results is excellent. Least squares fits to model (12) return the values $\Delta V = 0.35$ for $\varepsilon_{sl} = 0.3$, and $\Delta V = 0.32$ for $\varepsilon_{sl} = 0.6$ and 1. These results are remarkably consistent and also in good agreement with physical expectations, given the atomic volume size is of order $4\pi 0.5^3/3 = 0.52$. We also observe that these estimates suggest that $\partial \Delta V/\partial \varepsilon_{sl}$ is a small negative quantity. We will re-examine the validity of this interpretation in the following sections, in the light of additional simulation data that are independent of the data presented so far.

The middle panel of Fig. 1 compares MD simulation results for four temperatures. The agreement between the model and the simulation results is very good. The least squares fits return the values $\Delta V = 0.45$ for $T = 1.25$, $\Delta V = 0.32$ for $T = 2$ (as well as $T = 1.5$), and $\Delta V = 0.28$ for $T = 2.5$.
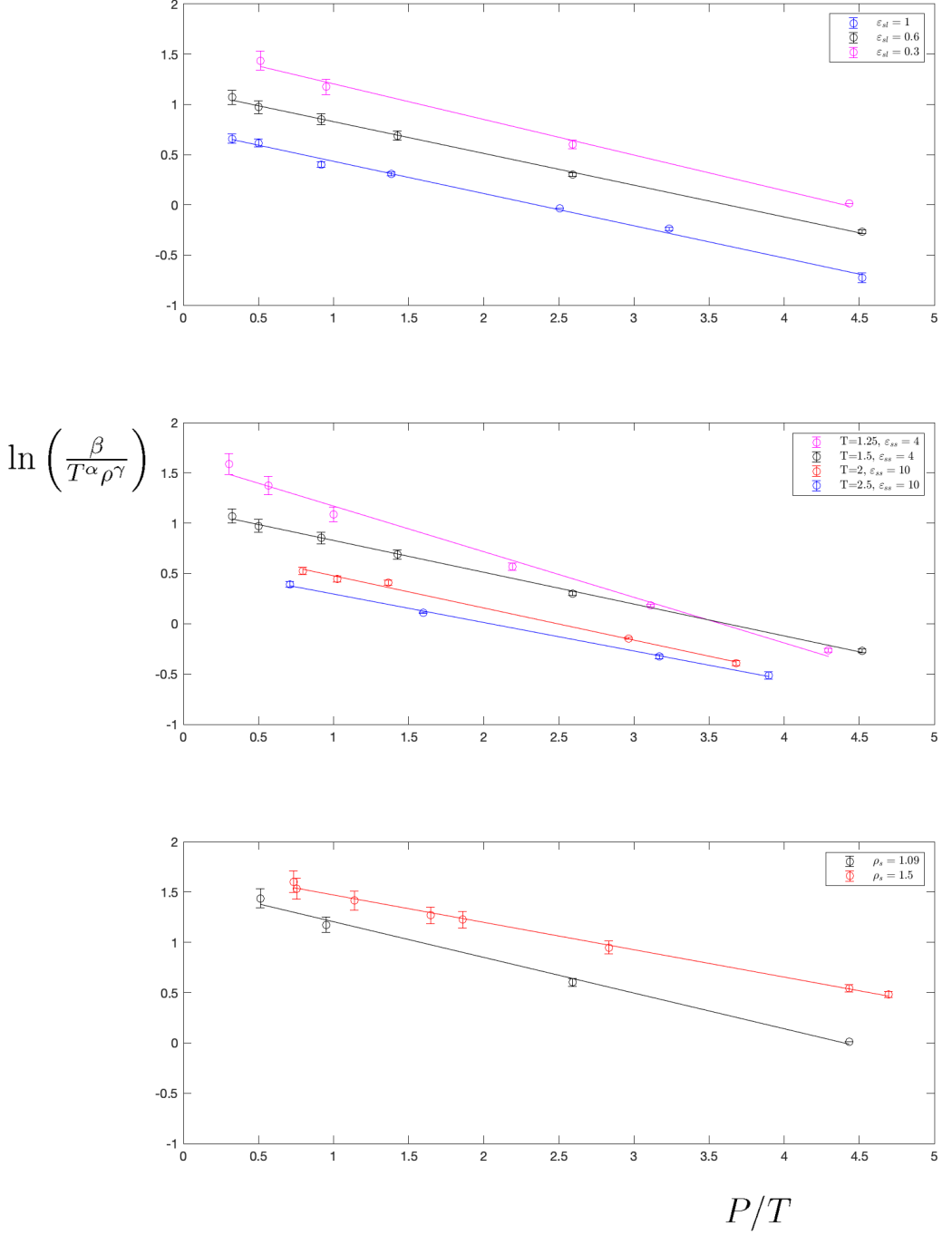
FIG. 1. MD simulation results for the slip length as a function of the ratio P/T, resulting from varying the liquid density in the range $0.53 < \rho < 0.92$ at fixed temperature. Solid lines indicate least-squares fits to model (12). Top: the effect of varying the solid-liquid interaction strength at fixed $T = 1.5$, $\varepsilon_{ss} = 4$, $\rho_s = 1.09$; middle: the effect of varying the temperature at fixed $\rho_s = 1.09$, $\varepsilon_{sl} = 0.6$; bottom: the effect of varying the solid density at fixed $T = 1.5$, $\varepsilon_{ss} = 4$, $\varepsilon_{sl} = 0.3$. For values of all other parameters see Appendix A.
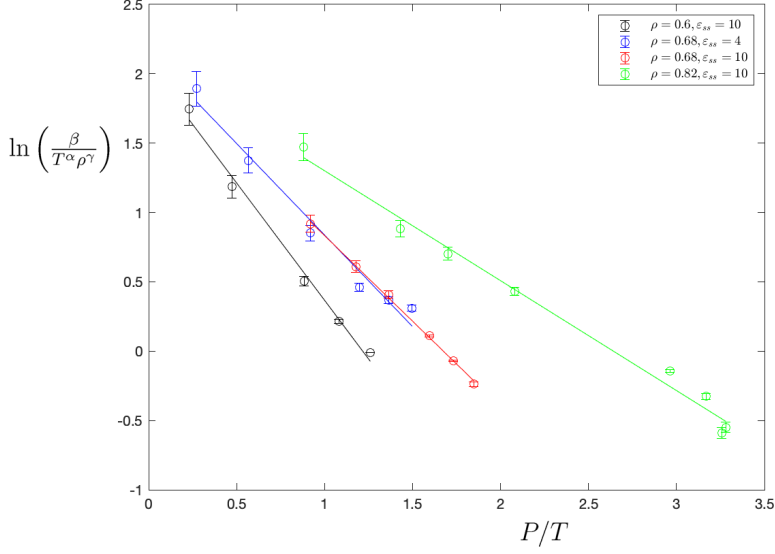
FIG. 2. MD simulation results as a function of P/T for $\varepsilon_{sl} = 0.6$ and $\varepsilon_{ss} = 10$ at three liquid densities: $\rho = 0.6$, $\rho = 0.68$, and $\rho = 0.82$. Results for $\rho = 0.68$ with $\varepsilon_{ss} = 4$ are also shown. Different values of P/T are obtained by varying the temperature. Solid lines indicate least-squares fits to model (13). For values of all other parameters see Appendix A.

With the exception of the case $T = 1.25$, these values are again remarkably consistent and seem to justify the assumption of weak temperature dependence.

The bottom panel of Fig. 1 investigates the effect of wall density, by considering two values of the latter; namely, the nominal density $\rho_s = 1.09$ and a higher density $\rho_s = 1.5$. The comparison is for $T = 1.5$, $\varepsilon_{sl} = 0.3$. The agreement with a least-squares fit to Eq. (12) is again excellent. The fit for $\rho_s = 1.5$ yields an estimate $\Delta V = 0.28$, which is close to the value $\Delta V = 0.35$ reported before for $\rho_s = 1.09$. We close by noting that since the mass ratio m_s/m_l has a very modest effect on slip, we expect it to have no effect on the qualitative aspects of our conclusions. To verify this, we repeated the simulations denoted by the black line in the middle panel of Fig. 1 with $m_s/m_l = 10$ instead of the nominal value $m_s/m_l = 5$; the results were indiscernible from the nominal case within the statistical uncertainty of our calculations.

2. Variation of slip with temperature at fixed density

In this section we present results obtained by varying the system temperature at fixed liquid density. Figure 2 shows results for the normalized slip length for $\varepsilon_{sl} = 0.6$, $\varepsilon_{ss} = 10$ and three values of the liquid density, namely $\rho = 0.6$, $\rho = 0.68$, and $\rho = 0.82$. Simulations for $\rho = 0.68$ were also performed with $\varepsilon_{ss} = 4$, primarily at lower temperatures. The comparison between the two values of ε_{ss} in Fig. 2 suggests that it has a small effect on the slip length.

Other than variable system temperature, these simulations were performed at the same values of all other parameters and are thus complementary to the simulations shown in the middle panel of Fig. 1. Substituting density with temperature as the independent variable provides a different perspective which is helpful for assessing the validity of our approximations about the dependence of ΔS, ΔV, and ΔU on ρ and T.

Figure 2 shows that, quite unexpectedly perhaps, the normalized slip is still well described by a model of the form

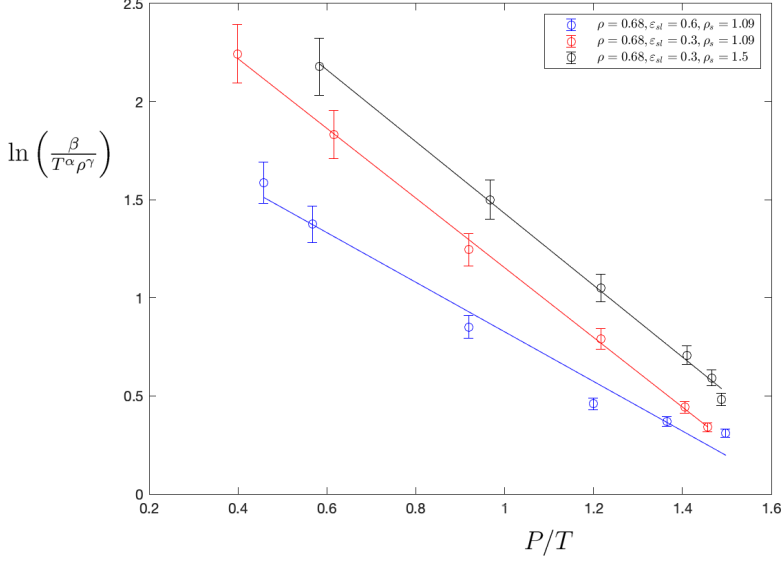$$\ln\left(\frac{\beta}{T^{\alpha}\rho^{\gamma}}\right) = \hat{c}_1 - \hat{c}_2 \frac{P}{k_B T}, \tag{13}$$

FIG. 3. MD simulation results as a function of P/T, showing the effect of solid-liquid interaction via different values of ε_{sl} and ρ_s. Different values of P/T are obtained by varying the temperature at constant liquid density. In all cases $\varepsilon_{ss} = 4$. The data for $\rho_s = 1.5$ was obtained by averaging data for $\rho = 0.65$ and $\rho = 0.71$ (at $\rho_s = 1.5$). Solid lines indicate least-squares fits to model (13).

where $\hat{c}_1$ and $\hat{c}_2$ are constants for the isochoric temperature sweeps considered in the figure. These constants can be related to c_1 and c_2 as we describe below.

We first note that $\hat{c}_1$ appears to be independent of density, while $\hat{c}_2 = \hat{c}_2(\rho)$; least squares fits return values $\hat{c}_1 = 2.06$, 2.06, 2.09 for $\rho = 0.6$, $\rho = 0.68$, and $\rho = 0.82$, respectively, for $\varepsilon_{ss} = 10$; for $\rho = 0.68$, $\varepsilon_{ss} = 4$ the fit value is $\hat{c}_1 = 2.16$. We also note that the liquid EOS in the range of conditions studied here can be approximated by the expression $P(\rho, T) \approx Ah(\rho)(T - T_0(\rho))$, where A is a system constant that does not depend on ε_{sl}, while $h(\rho)$, $T_0(\rho)$, and $dh/d\rho$ are positive functions of ρ. Let us finally write $\Delta S = \Delta S_0 + \Delta S_{\varepsilon_{sl}}$, where $\Delta S_{\varepsilon_{sl}}$ denotes the part of ΔS that explicitly depends on ε_{sl}, while ΔS_0 denotes the remainder that does not. Using the above EOS and identifying AT_0/T with $(T\Delta S_0 - \Delta U)/T$ in (10), leads to an expression of the form

$$\ln\left(\frac{\beta}{T^\alpha \rho^\gamma}\right) = B' - \frac{P}{k_B T}\left(\Delta V + \frac{1}{h(\rho)}\right), \tag{14}$$

where $B' = B + (A + \Delta S_{\varepsilon_{sl}})/k_B$ is a system constant (neglecting any dependence of $\Delta S_{\varepsilon_{sl}}$ on ρ or T). This relation, although approximate, is consistent with (13) and correctly predicts the increase in slope $\hat{c}_2 > c_2$, as well as the dependence of this increase on the liquid density.

Figure 3 shows additional slip data obtained by varying the temperature at fixed density, exploring the effect of wall density and solid-liquid interaction strength. The result for $\rho = 0.68$, $\varepsilon_{ss} = 4$, $\varepsilon_{sl} = 0.6$, already discussed in Fig. 2 is included for reference purposes. The figure shows that the data is fitted well by the general form of relation (13). We also note that the two results for $\rho_s = 1.09$ are consistent with our previous finding that $\partial \Delta V/\partial \varepsilon_{sl}$ is a small negative quantity.

Connection with previous work. In this section we try to place the above results in the context of previous work [22] which found, albeit for a slightly different system, that slip data as a function of temperature at fixed density can be collapsed by an expression of the form $\beta \propto \exp(H/T)$ with $H > 0$ dependent on density. We first observe that the above form, namely $\beta \propto \exp(H/T)$ with $H > 0$, is likely a derived relation since it lacks the signature negative sign in the exponent. We also
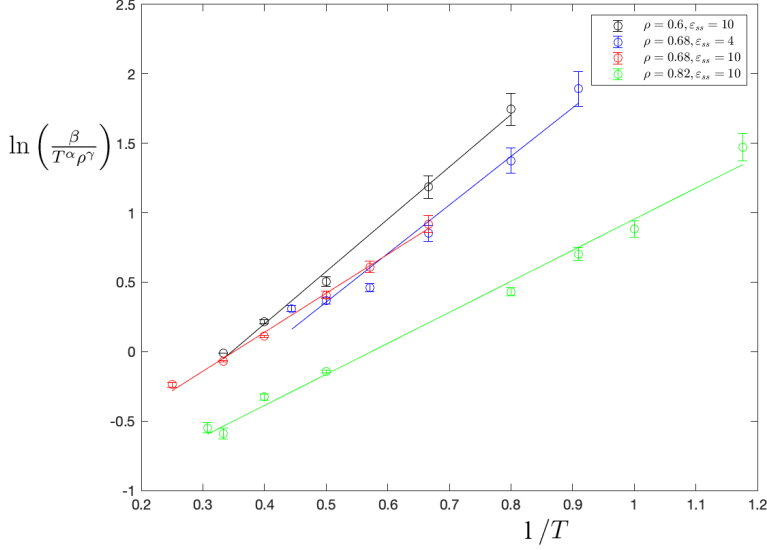
FIG. 4. MD simulation results shown in Fig. 2 plotted as a function of $1/T$. Results for three liquid densities are shown: $\rho = 0.6$, $\rho = 0.68$, and $\rho = 0.82$ for $\varepsilon_{sl} = 0.6$ and $\varepsilon_{ss} = 10$. Results for $\rho = 0.68$ with $\varepsilon_{ss} = 4$ are also shown. Solid lines indicate least-squares fits to model (15).

observe that using the EOS $P(\rho, T) \approx Ah(\rho)(T - T_0(\rho))$, relation (14) can be written in the form

$$\ln\left(\frac{\beta}{T^\alpha \rho^\gamma}\right) = D(\rho) + \frac{E(\rho)}{k_B T}, \tag{15}$$

where $D(\rho)$ and $E(\rho)$ are functions of density (in addition to $\{\phi\}$). In taking this step we have neglected the dependence of ΔV on temperature, as we have done throughout Sec. III B.

Since on physical grounds we expect $\Delta V > 0$, we can expect $E(\rho) > 0$ as found in [22]. In other words, at least for the system studied here and within the accuracy of the approximate form of the EOS used above, relations (14) and (15) should be equivalent.

Figure 4 validates this assertion by replotting the data shown in Fig. 2 in a form consistent with relation (15), namely normalized slip as a function of $1/T$ for a liquid of fixed density. Fits to the data using (15) for each density are also shown. The agreement between MD data and the fits is comparable to that shown in Fig. 2; this observation is supported by comparable least-squares residuals. In other words, both relations (14) and (15) appear to fit the data satisfactorily.

Figure 5 provides additional validation by plotting the data of Fig. 3 as a function of $1/T$. Fits to relation (15) again verify that both relations (14) and (15) fit the data satisfactorily.

3. Slip as a function of ε_{sl}

Figure 6 shows MD simulation results for the slip length as a function of ε_{sl}. The simulations are performed at constant temperature $T = 1.5$, for two liquid densities, namely $\rho = 0.68$ and $\rho = 0.825$.

Neglecting the dependence of ΔV on ε_{sl} based on our previous observations that $\partial \Delta V / \partial \varepsilon_{sl}$ is a small quantity, to a first order approximation, we can write (10) in the form

$$\ln(\beta) = \hat{B} + \frac{1}{k_B} \frac{\partial\left(Bk_B + \Delta S_{\varepsilon_{sl}}\right)}{\partial \varepsilon_{sl}}\bigg|_{\varepsilon_{sl}^{\text{ref}}} \varepsilon_{sl}, \tag{16}$$
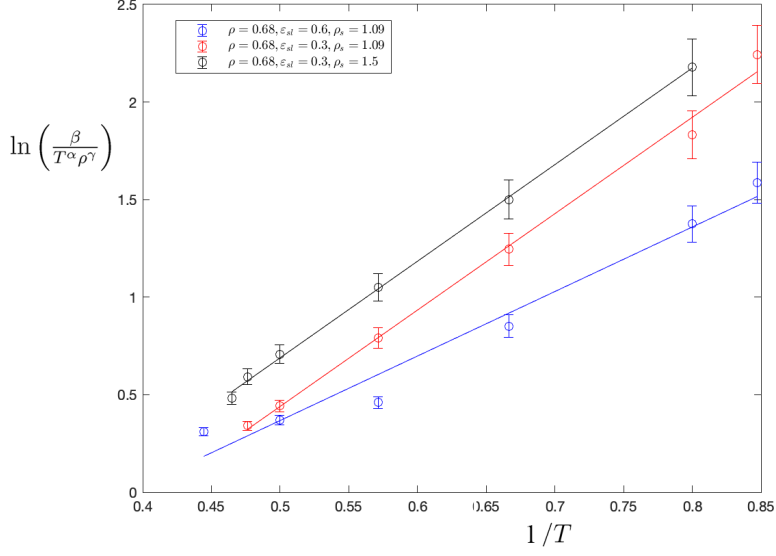
FIG. 5. MD simulation results shown in Fig. 3 plotted as a function of $1/T$. Solid lines indicate least-squares fits to model (15).

where, from (14), $\hat{B} = [A + (Bk_B + \Delta S_{\varepsilon_{sl}})|_{\varepsilon_{sl}^{\mathrm{ref}}}]/k_B - P[\Delta V + 1/h(\rho)]/k_B T$ and thus constant for the isothermal-isochoric simulations considered here, and $\varepsilon_{sl}^{\mathrm{ref}}$ denotes the reference point about which the dependence of $Bk_B + \Delta S_{\varepsilon_{sl}}$ on ε_{sl} is linearized. This relation implicitly assumes that ΔU does not depend on ε_{sl}, or at least its dependence on ε_{sl} is negligible compared to that of $Bk_B + \Delta S_{\varepsilon_{sl}}$; this is the simplest model we can propose which explains the behavior observed in the
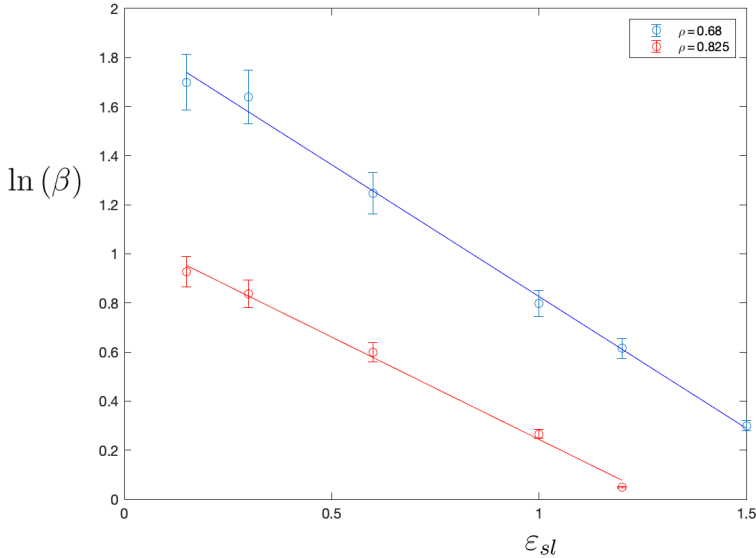

FIG. 6. MD simulation results for the slip length dependence on the solid-liquid interaction parameter ε_{sl} for $T = 1.5$ and two liquid densities: $\rho = 0.68$ and $\rho = 0.825$. Solid lines indicate least-squares fits of a linear model to the data. For values of all other parameters see Appendix A.

figure—namely, linear dependence of $\ln(\beta)$ on ε_{sl}—without introducing any inconsistencies in our previous models. For example, a dependence of ΔU on ε_{sl} prevents (14) following from (10).

Given Eq. (16), from Fig. 6 we conclude that $[\partial(Bk_B + \Delta S_{\varepsilon_{sl}})/\partial\varepsilon_{sl}]|_{\varepsilon_{sl}^{\mathrm{ref}}} < 0$. This is consistent with the behavior observed in Fig. 3 and the top panel of Fig. 1, where the variation in the ordinate intersept can be identified with $B + \Delta S_{\varepsilon_{sl}}/k_B$.

IV. DISCUSSION AND CONCLUSIONS

Using the Eyring theory of reaction rates we have developed an expression for the slip length of a simple liquid in contact with a simple solid boundary. Our work focuses on the limit of linear conditions (small shear rate) which, as discussed in Sec. II, covers essentially all practical applications of interest.

The resulting model is validated by an extensive comparison with MD simulation data of slip in the linear regime. The comparison with MD data reveals remarkably good agreement with the expected Arrhenius behavior, provided pre-exponential factors, as well as the dependence of the activation free energy on the system state, are taken into account.

Using the simplest, perhaps, model that is consistent with our data to interpret the latter, we find that, at constant temperature, the activation free energy depends linearly on pressure, the latter being a direct result of the $P\Delta V$ term, where ΔV may be interpreted as the volume change associated with a hole creation. Under variable temperature conditions and fixed density we find that either of $1/T$ and P/T can be used as an independent variable for Arrhenius-type plots; the former leads to plots of positive slope. This is shown to be a result of the interplay between various terms in the expression for the activation free energy and the liquid equation of state. In other words, the $1/T$ behavior is not a result of a fundamentally simple behavior, such as a constant activation energy.

Although some of the findings summarized above may be specific to the solid-liquid system considered here, the excellent agreement with the MD data, as well as the very reasonable values for the model parameters used to fit the data suggest that the thermally activated model for slip is not only reasonable but also reliable in the linear regime. In particular, the improved agreement with the MD data achieved after accounting for a number of subtle physical effects, such as distinguishing between slip at the FLL and GK slip, increases our confidence in the physical underpinnings of the model.

Completing this approach to describing slip requires a more rigorous characterization of the effect of system parameters, such as wall density and structure, etc., on the activation free energy and ultimately slip. This will be undertaken in future work efforts.

APPENDIX A: MOLECULAR SIMULATION SETUP

We performed Couette flow simulations in a system comprising a dense liquid bounded by two fcc-structured walls in a slab geometry. Our simulations were performed using the LAMMPS software [33].

A schematic of the simulated system is shown in Fig. 7. The domain has dimensions $L_x = L_y = 30.8$ LJ units in each of the two directions parallel to the walls; the transverse dimension available to the liquid (distance between the walls) was $L \approx 30$ LJ units (varied slightly with pressure and temperature). Depending on the liquid density, the number of liquid particles varied between 16 000 and 25 000.

Each wall consisted of a 7.71 unit thick FCC slab of atoms divided into three regions, each under different dynamics. The outermost region contained three atomic layers frozen relative to each other and translating with velocity $\pm U$ in the x direction (shown in blue color in the figure). The middle region contained seven atomic layers thermostated to the desired system temperature (T) via a Nosé–Hoover thermostat (shown in red in the figure). The innermost region (shown as brown in the figure), in contact with the liquid, comprised of a single atomic layer under NVE dynamics. The surface of the wall exposed to the liquid is the (0,0,1) plane of the FCC crystal.
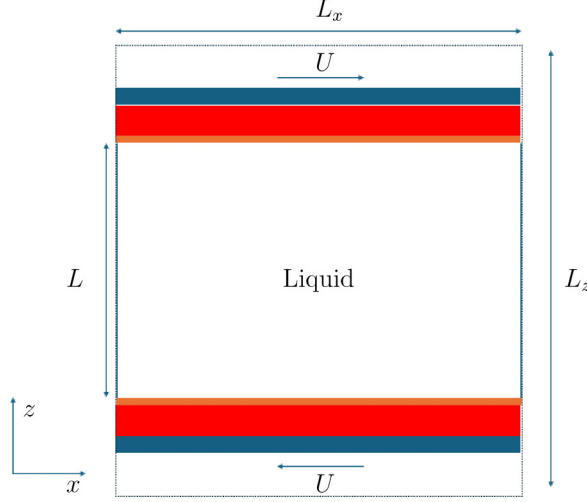
FIG. 7. Schematic of the simulation domain. The dashed line outlines the simulation box over which periodic boundary conditions are applied in all directions; $L_z = 77.1$ denotes the size of the simulation domain in the z direction.

All nonfrozen interactions were modeled using the Lennard-Jones potential given in Eq. (11). Unless otherwise stated, the nominal wall density was fixed at $\rho_s = 1.09$, with $m_s = 5$ ($m_l = 1$), $\sigma_{ss} = 1$ ($\sigma_{ll} = 1$), and $\varepsilon_{ss} = 4$ ($\varepsilon_{ll} = 1$). In all our simulations $C_{ss} = C_{ll} = 1$ and $C_{sl} = 0.6$. A potential cutoff of 5 LJ units was used. Periodic boundary conditions were used throughout (the wall thickness was much larger than the potential cutoff).

APPENDIX B: SLIP DEFINITION AND MEASUREMENT

Our Couette flow simulations were performed at wall speeds of $U = \pm 0.1$ in LJ units (σ / τ_{LJ}). This magnitude is sufficiently small for nonlinear effects and viscous heating to be negligible (maximum temperature variation across the fluid was less than 0.01).

The slip length was measured using both the nonequilibrium definition, namely as the distance into the wall at which the extrapolated fluid velocity profile reaches the wall speed value, and the equilibrium definition [9], namely using the GK relation

$$\beta_{GK} = \frac{\mu A k_B T}{\int_0^\infty \langle F_i(t) F_i(0) \rangle dt}, \tag{B1}$$

where $A = L_x L_y$ denotes the solid-liquid interface area and $F_i(t)$ is the force the liquid exerts on the solid in a direction parallel to the interface ($i \in \{x, y\}$). In our calculations, data was averaged over both the x and y directions.

In the nonequilibrium case, the velocity gradient was calculated using a linear approximation of the velocity profile fitted over the middle 95% of the liquid domain, away from the layering present close to the walls. To achieve the desired statistical uncertainty [34], the velocity profile was averaged over 5×10^6 timesteps following an equilibration period of 5×10^6 timesteps.

Due to the known plateau problem [9] in evaluating GK integrals of the type found in (B1), β_{GK} is calculated using the method by Oga et al. [35]. The calculation was performed using MD trajectories of length 10^6 timesteps after an equilibration period of 10^7 timesteps.

As discussed in Ref. [10], the equilibrium and nonequilibrium measurements of slip are equivalent, provided the hydrodynamic wall location associated with the Green-Kubo result is properly taken into account. In this work, the hydrodynamic wall location, z_{GK}^w was calculated using the

force-balance approach outlined in [10]. The two methods of measurement were found to yield consistent results. In the results in Sec. III B the value of β reported is $\beta_{GK} - z_{GK}^w + z_0$, where $z_0 = 0.8$ represents the nominal distance between the wall and the FLL layer [2,8,36]. In other words, by correcting the Green-Kubo slip length for the distance between the hydrodynamic wall location and the FLL, we have an estimate for the slip length at the FLL that can be directly compared with the prediction of Eq. (10).

---

[1] M. Navier, Sur les Lois du Mouvement des Fluides, Mémoires L'Académie des Sci. L'institut Fr. **6**, 389 (1823).

[2] N. G. Hadjiconstantinou, Molecular mechanics of liquid and gas slip flow, Annu. Rev. Fluid Mech. **56**, 435 (2024).

[3] N. G. Hadjiconstantinou, The limits of Navier-Stokes theory and kinetic extensions for describing small-scale gaseous hydrodynamics, Phys. Fluids **18**, 111301 (2006).

[4] Y. Sone, *Molecular Gas Dynamics: Theory, Techniques, and Applications* (Birkhauser, 2007).

[5] J. L. Barrat and L. Bocquet, Influence of wetting properties on hydrodynamic boundary conditions at a fluid/solid interface, Faraday Discuss. **112**, 119 (1999).

[6] K. Falk *et al.*, Molecular origin of fast water transport in carbon nanotube membranes: Superlubricity versus curvature dependent friction, Nano Lett. **10**, 4067 (2010).

[7] C. Sendner *et al.*, Interfacial water at hydrophobic and hydrophilic surfaces: Slip, viscosity, and diffusion, Langmuir **25**, 10768 (2009).

[8] G. J. Wang and N. G. Hadjiconstantinou, Molecular mechanics and structure of the fluid-solid interface in simple fluids, Phys. Rev. Fluids **2**, 094201 (2017).

[9] L. Bocquet and J.-L. Barrat, Hydrodynamic boundary conditions, correlation functions, and Kubo relations for confined fluids, Phys. Rev. E **49**, 3079 (1994).

[10] N. G. Hadjiconstantinou and M. M. Swisher, On the equivalence of nonequilibrium and equilibrium measurements of slip in molecular dynamics simulations, Phys. Rev. Fluids **7**, 114203 (2022).

[11] S. Lichter, A. Roxin, and S. Mandre, Mechanisms for liquid slip at solid surfaces, Phys. Rev. Lett. **93**, 086001 (2004).

[12] A. Martini *et al.*, Molecular mechanisms of liquid slip, J. Fluid Mech. **600**, 257 (2008).

[13] N. G. Hadjiconstantinou, An atomistic model for the Navier slip condition, J. Fluid Mech. **912**, A26 (2021).

[14] P. Hänggi, P. Talkner, and M. Borkovec, Reaction-rate theory: fifty years after Kramers, Rev. Mod. Phys. **62**, 251 (1990).

[15] T. D. Blake and J. M. Haynes, Kinetics of liquid/liquid displacement, J. Col. Int. Sci. **30**, 421 (1969).

[16] T. D. Blake *et al.*, Contact angle relaxation during droplet spreading: Comparison between molecular kinetic theory and molecular dynamics, Langmuir **13**, 2164 (1997).

[17] T. D. Blake and J. De Coninck, The influence of solid-liquid interactions on dynamic wetting, Adv. Col. Int. Sci. **96**, 21 (2002).

[18] J. De Coninck and T. D. Blake, Wetting and molecular dynamics simulations of simple liquids, Annu. Rev. Mater. Res. **38**, 1 (2008).

[19] M. J. de Ruijter, T. D. Blake, and J. D. Coninck, Dynamic wetting studied by molecular modeling simulations of droplet spreading, Langmuir **15**, 7836 (1999).

[20] T. D. Blake, Dynamic contact angles and wetting kinetics, in *Wettability*, edited by J. C. Berg (Marcel Dekker, Inc., New York, Basel, Hong Kong, 1993), pp. 251–309.

[21] T. D. Blake and J. De Coninck, Dynamics of wetting and Kramers' theory, Eur. Phys. J. Spec. Top. **197**, 249 (2011).

[22] S. Lichter *et al.*, Liquid slip in nanoscale channels as a rate process, Phys. Rev. Lett. **98**, 226001 (2007).

[23] B. Shan *et al.*, Molecular kinetic modelling of nanoscale slip flow using a continuum approach, J. Fluid Mech. **939**, A9 (2022).

[24] G. J. Wang and N. G. Hadjiconstantinou, Universal molecular-kinetic scaling relation for slip of a simple fluid at a solid boundary, Phys. Rev. Fluids **4**, 064201 (2019).

[25] R. B. Bird, W. E. Stewart, and E. N. Lightfoot, *Transport Phenomena* (Wiley, New York, 2002).

[26] S. Glasstone, K. Laidler, and H. Eyring, *The Theory of Rate Processes* (McGraw-Hill, New York, 1941).

[27] J. I. Frenkel, *Kinetic Theory of Liquids* (Oxford University Press, Oxford, 1946).

[28] D. M. Tolstoi, Molecular theory for slippage of liquids over solid surfaces, Doklady Acad. Nauk SSSR **85**, 1089 (1952).

[29] T. D. Blake, Slip between a liquid and a solid: D. M. Tolstoi's (1952) theory reconsidered, Colloids Surf. **47**, 135 (1990).

[30] N. V. Priezjev, Rate-dependent slip boundary conditions for simple fluids, Phys. Rev. E **75**, 051605 (2007).

[31] P. A. Thompson and S. M. Troian, A general boundary condition for liquid flow at solid surfaces, Nature (London) **389**, 360 (1997).

[32] J. K. Johnson, J. A. Zollweg, and K. E. Gubbins, The Lennard-Jones equation of state revisited, Mol. Phys. **78**, 591 (1993).

[33] S. Plimpton, Fast parallel algorithms for short-range molecular dynamics, J. Comput. Phys. **117**, 1 (1995).

[34] N. G. Hadjiconstantinou *et al.*, Statistical error in particle simulations of hydrodynamic phenomena, J. Comput. Phys. **187**, 274 (2003).

[35] H. Oga *et al.*, Green-Kubo measurement of liquid-solid friction in finite-size systems, J. Chem. Phys. **151**, 054502 (2019).

[36] G. J. Wang and N. G. Hadjiconstantinou, Why are fluid densities so low in carbon nanotubes? Phys. Fluids **27**, 052006 (2015).